Smart Structures and Systems, *Vol. 35, No. 5 (2025) 253-265*
https://doi.org/10.12989/sss.2025.35.5.253

The performance of neural-evolutionary optimization approaches' efficiency in forecasting belled piles' pullout capacity

Chao Liu [1a], Hossein Moayedi[*2,3] and Xiang Zhang [1b]

[1] *School of Smart Urban Construction, Guangzhou City Polytechnic, Guangzhou, 510370, China*
[2] *Institute of Research and Development, Duy Tan University, Da Nang, 550000, Vietnam*
[3] *Faculty of Civil Engineering, Duy Tan University, Da Nang 550000, Vietnam*

(*Received May 22, 2022, Revised April 10, 2024, Accepted June 17, 2025*)

Abstract. The primary objective of this study is to predict the pullout capacity of belled piles by developing and evaluating various hybrid modeling techniques, including Evolution Strategy (ES), Moth Flame Optimizer (MFO), Grasshopper Optimization Algorithm (GOA), and League Championship Algorithm (LCA). Each hybrid model combines an artificial neural network (ANN) with an optimization algorithm, trained using a hybrid learning approach that incorporates back-propagation and least squares estimation, implemented in MATLAB. A total of 36 samples were used, with 25 designated for training and 11 for testing. The performance of each model was assessed using statistical metrics, namely the coefficient of determination (R^2) and root mean square error (RMSE). Among the models, MFO-ANN demonstrated the highest predictive accuracy, followed by LCA-ANN, ES-ANN, and GOA-ANN, respectively. The results confirm the robustness and reliability of the ANN-based hybrid models in estimating pullout capacity.

Keywords: belled piles; machine learning; metaheuristic modelling; pullout behavior

1. Introduction

High-rise structures, such as mooring systems on the water surface, transmission towers, and high-rise buildings, are subjected to significant lateral forces and substantial overturning moments caused by wind, waves, or a combination of both, in addition to vertical compressive loads, To enhance the load-bearing capacity of deep foundations, enlarged base piles made of concrete have been developed, featuring an inverted cone-shaped base to improve their performance. Various computational models have been employed to investigate the behavior of these piles under varying conditions and variables. Intelligent techniques have been increasingly applied in pile engineering for a variety of purposes, such as designing piles under varying load types and directions (Sego *et al*. 2003, Amjad *et al*. 2022), predicting the bearing capacity of pile foundations (Consoli *et al*. 2017, Zhu *et al*. 2017, Kumar and Choudhury 2018), estimating the uplift capacity of suction caissons (Tu *et al*. 2020), assessing dynamic load capacity (Dong and Zheng 2015, Prendergast and Gavin 2016), optimizing pile configurations (Ottolini *et al*. 2015, Zhang and Wang 2015), and evaluating pile settlements (Fleming 1992).

As previously mentioned, belled piles—constructed from concrete—are specifically designed to enhance the bearing capacity of embedded piles. These types of piles are suitable for use in both cohesive and non-cohesive soils, featuring a base geometry that is intentionally shaped as an inverted cone. Ashour and Ardalan (2011) applied the Group Method of Data Handling (GMDH), a neural network-based technique, along with genetic algorithm (GA), to examine the influence of cone point resistance and sleeve friction on the unit shaft resistance of piles. Moreover, Li *et al*. (2020) introduced Tree-based Genetic Programming (TGP) as an effective method for predicting pile behavior.

Linear Genetic Programming (LGP) and Gene Expression Programming (GEP) have been employed to improve prediction equations for estimating the pullout capacity of suction caissons using datasets derived from existing literature. The application of Adaptive Neuro-Fuzzy Inference Systems (ANFIS) in geotechnical engineering was thoroughly discussed by Cabalar *et al*. (2012). Similarly, Nazir *et al*. (2015) demonstrated the effectiveness of combining the Imperialist Competitive Algorithm with Artificial Neural Networks (ICA-ANN) to predict the uplift resistance of screw piles. Yilmaz *et al*. (2012) investigated the application of artificial neural networks (ANNs) and adaptive neuro-fuzzy inference systems (ANFIS) for predicting the permeability of coarse-grained soils. Another notable study by Sadeghiamirshahidi and Ardejani (2013) utilized neural networks to predict the oxidation potential of pyrite in specific types of refuse piles, showing the broad applicability of machine learning in geotechnical assessments.

Zhao *et al*. (2025) highlighted that the stress path method provides critical insight into the evolution of soil

*Corresponding author, Ph.D.,
E-mail: hosseinmoayedi@duytan.edu.vn
[a] Ph.D., E-mail: superenzo@gcp.edu.cn
[b] Ph.D., E-mail: zhangxiang1994@gcp.edu.cn

ISSN: 1738-1584 (Print), 1738-1991 (Online)

stress states under loading, which directly influences the bearing capacity and load-settlement behavior of piles in geotechnical design. Yao *et al*. (2023) mentioned the study of cyclic performance in composite beam-to-column connections require understanding of energy dissipation and deformation behavior under cyclic loading to ensure structural resilience as similar to the pile design. Yao *et al*. (2022) investigated on the seismic performance insights from steel-PEC spliced frame beams which can inform pile bearing capacity analysis by enhancing the understanding of load transfer, ductility, and structural response under dynamic loading conditions. In addition, the study on the reasonable width of narrow coal pillars under a hard primary roof provides valuable insights into load distribution, confinement effects, and stability mechanisms in deep underground conditions. These concepts are directly relevant to pile bearing capacity, as both involve understanding how subsurface materials respond to concentrated loads and maintain structural integrity under high stress environments (Meng *et al*. 2024). Discrete element analysis offers a powerful tool for simulating soil–structure interaction at the particle level, enabling a more detailed understanding of load transfer mechanisms and failure patterns that directly influence pile bearing capacity or even tunnel deformation behavoiur (Chang *et al*. 2024, Wang *et al*. 2024a, b, Hu *et al*. 2025). On the other hand, Understanding pile–soil interaction is essential for accurately predicting pile bearing capacity, as it governs how loads are transferred from the pile to the surrounding soil and directly influences settlement, stability, and overall foundation performance (Huang *et al*. 2021, Wang *et al*. 2024c, Hua *et al*. 2025). Understanding the microstructural evolution and mechanical properties of snow under compression provides valuable insights into the behavior of weak or porous geomaterials, which is critical for accurately assessing pile bearing capacity in cold regions with snow or permafrost-influenced ground conditions (Ma *et al*. 2025). Niu *et al*. (2024) suggested plastic damage prediction of concrete under compression using deep learning is relevant to pile bearing capacity design, as it enhances the ability to model and predict material degradation, which is crucial for assessing the long-term performance and reliability of pile foundations in concrete structures. Wang *et al*. (2024d) investigated on the topology optimization of active tensegrity structures contributes to pile bearing capacity design by offering advanced methods to optimize structural frameworks, potentially improving load distribution and adaptability in foundation systems under complex loading conditions. In addition, the comparison of inter-storey isolation and base isolation using friction pendulum systems informs pile bearing capacity design by enhancing understanding of how seismic isolation techniques influence dynamic load transfer to foundations, thereby affecting pile performance and stability during earthquakes (Zhang *et al*. 2024, 2025). Zhou *et al*. (2022) investigates the mechanical behavior and thermal degradation mechanisms of granite under coupled high-temperature and high-pressure conditions, revealing that increased temperature reduces strength and elasticity primarily through thermal cracking and friction weakening, while deformation is mainly controlled by confining pressure.

Furthermore, Wu *et al*. (2013) proposed an analytical model for a single axially loaded bored pile, incorporating a nonlinear soft computing approach (Liu *et al*. 2020b). They noted that the soft characteristics of skin friction in bored piles were not accurately modeled under low-load conditions. Xiao *et al*. (2012) investigated pile integrity using low-strain testing techniques and implemented a Backpropagation (BP) neural network algorithm for analysis. Thomas *et al*. (2016) introduced a randomized adaptive neuro-fuzzy inference system (ANFIS) model to forecast seismic ground motion parameters.

Ganjidoost *et al*. (2016) employed a hybrid approach combining ANFIS with Genetic Algorithms (GAs) to predict the soil permeability coefficient. The effectiveness of ANFIS in estimating the resilient modulus of subgrade soils in flexible pavements was also demonstrated by Sadrossadat *et al*. (2016). Similarly, Momeni *et al*. (2015) reported promising results using neural networks for predicting the ultimate bearing capacity of precast reinforced concrete piles.

Further research by Moayedi and Rezaei (2019) focused on predicting the uplift forces on under-reamed piles using artificial neural networks (ANNs), achieving high prediction accuracy. Liu *et al*. (2020a) introduced a novel methodology for estimating lateral displacements resulting from pile installation. Wu *et al*. (2013) employed numerical simulations to investigate pile bearing behavior, taking into account the crushing of sand particles. Liu *et al*. (2020a) conducted numerical modeling to assess the setup effects around the shaft of XCC piles in clayey soils. Lastly, Cui *et al*. (2018) explored the dynamic response of pipe piles embedded in layered viscoelastic media with radial inhomogeneity under vertical excitation, contributing to a deeper understanding of pile behavior in complex subsurface conditions. Chisari *et al*. (2015) applied a Genetic Algorithm (GA)-based inverse identification technique to a base-isolated, post-tensioned concrete bridge, utilizing in-situ static and dynamic test data, which enabled the accurate estimation of material properties and isolator stiffness. The GA approach outperforms traditional methods by enabling the identification of multiple parameters and achieving a strong correlation with finite element model updates, thereby demonstrating its potential for broader structural applications.

This study presents a reliable prediction model for estimating the pullout capacity of belled piles embedded in coarse-grained soils using advanced optimization algorithms. The input parameters considered include the enlarged base angle, base diameter, embedment ratio, and shaft diameter, while the pullout capacity of the belled pile serves as the output variable. The structure of article is organized as follows: (i) the Introduction outlines the relevant literature and highlights the significance of the research; (ii) the Methodology details five proposed hybrid models that integrate ANNs with optimization algorithms—ES-ANN, MFO-ANN, GOA-ANN, and LCA-ANN; (iii) the Data Collection and Model Evaluation section describes the preparation of training and testing datasets, as well as

the application of machine learning techniques for model training. This section also presents preliminary performance comparisons among the five hybrid models. Finally, (iv) the Network Performance section identifies the best-performing hybrid model and provides comparative plots of actual versus predicted pullout capacities (Pu).

2. Established databases

In this study, a limited dataset derived from the small-scale laboratory tests conducted by Nazir *et al*. (2015) was utilized. The input parameters for the ANFIS model, consistent with the experimental setup, included: (1) enlarged base angles of 30°, 45°, and 60°, (2) shaft diameters (Ds) of 30, 40, and 50 mm, (3) base diameters (D_b) of 75, 100, 125, and 150 mm, and (4) embedment ratios (L/Db) of 1, 2, 3, 4, and 5. The output parameter was the pullout load (Pu). The uplift resistance values used in the model were obtained directly from Nazir *et al*. (2015) experimental work, as summarized in Table 1. Fig. 1 illustrates the experimental setup and parameter configuration.

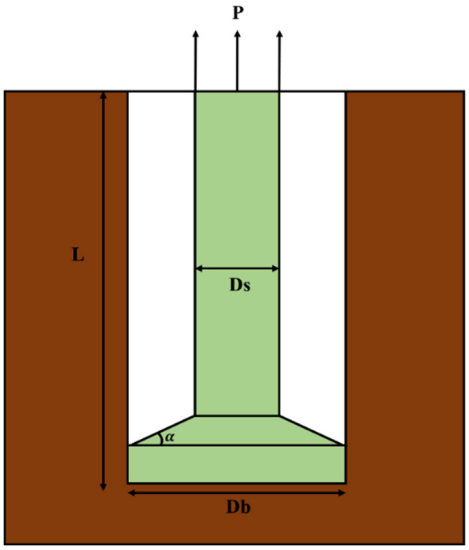

Fig. 1 A sample of the enlarged base pile and critical parameters for modeling, F is pullout load, Ds is shaft diameter, L is pile length, α is bell angle, and Db is the base diameter

Table 1 Physical amounts of the uplift resistance within the artificial neural network (ANN) and laboratory work

Material Property	Values	Symbol	Units
Pile			
Shaft diameter	30-40-50	Ds	mm
Base diameter	75-100-125-125	Db	mm
Embedment ratio	0-1-2-3-4-5	L/Db	-
Base angle	30-45-60	α	°
Soil			
Relative density	Dense-85% Loose-35%	Id	
Dry unit weight	14.7, 18.0	Yd	%

3. Methodology

To evaluate the effectiveness of hybrid neural-evolutionary models in predicting the pullout capacity of belled piles, a structured methodology was followed that involved data preparation, model development, training, and performance assessment. The investigation utilized a dataset comprising 36 experimental samples obtained from controlled laboratory tests. These samples included key input parameters influencing pile behavior, such as shaft diameter (Ds), enlarged base diameter (Db), soil density, and embedment ratio (L/Db). The importance of incorporating additional influential parameters, such as Young's modulus, which can significantly enhance the accuracy of bearing capacity predictions, is known. While this parameter was not included in the current model due to limitations in the available dataset, we agree that its inclusion in future studies would strengthen the robustness and generalizability of the predictive models (Chisari *et al*. 2015). Note that out of the total dataset, 25 samples were used for model training and 11 for testing, based on a 70/30 split.

The core of the study involved coupling ANN with four distinct optimization algorithms: ES, MFO, GOA, and LCA. These hybrid models (ES-ANN, MFO-ANN, GOA-ANN, and LCA-ANN) were developed using a hybrid learning strategy that combined backpropagation with least squares estimation, enabling improved convergence and enhanced generalization performance. All modeling and simulations were performed using MATLAB.

Each optimization algorithm was used to tune the neural network's parameters, such as weights, biases, and learning rates, to minimize the prediction error. The performance of each hybrid model was quantitatively assessed using two widely accepted statistical metrics: the coefficient of determination (R^2) and root mean square error (RMSE). These metrics provided insights into both the accuracy and reliability of the model's predictions against actual measured values.

By utilizing swarm-based and evolutionary algorithms to enhance the neural network's learning process, the study aimed to address the limitations of traditional artificial neural networks (ANNs), particularly in small-sample geotechnical applications. Comparative analysis across the four hybrid approaches enabled a ranking of model effectiveness, which served as the basis for further discussion and conclusion.

3.1 Artificial Neural Network

Artificial Neural Networks (ANNs) are powerful tools for modeling complex systems in various fields, including medicine, finance, and engineering. They function by simulating the structure and processes of the human brain, utilizing an intricately interconnected multi-layer structure composed of numerous neurons. This network is capable of

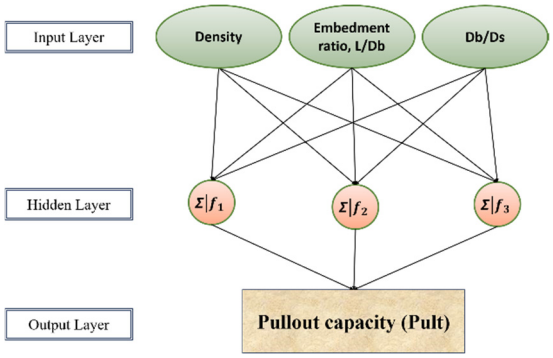

Fig. 2 Structure of the ANN used in this study

recognizing patterns and making predictions, especially when exposed to new input data after being properly trained to predict the desired output. ANNs are often used as an alternative to complex statistical analysis methods, such as autocorrelation, trigonometric functions, multivariable regression, and linear regression. A typical ANN is defined by three fundamental components: (1) transfer function, (2) network architecture, and (3) learning law (e.g., Buses). These elements are crucial for selecting the most suitable model for a specific problem (Fig. 2). Over time, various algorithms have been developed to train neural networks, with feedforward neural networks (FFNN) and the back-propagation (BP) algorithm being among the most reliable and effective techniques. BP, in particular, is widely used to solve complex predictive geotechnical problems, which contributes to its popularity for training artificial neural networks (ANNs).

3.2 Evolution strategy

The ES was initially developed by Rechenberg (1984) to solve optimization problems based on the natural mechanisms of evolution that occur in species in nature. In each generation, new individuals are generated from the individuals present in the parent population, constituting the offspring population. Like GA, the ES works with populations of candidate solutions, requiring only data based on the objective function and constraints, without the need for derivatives or another auxiliary knowledge. However, ES works directly with the real representation of the decision variables (in this case, a set of geomechanical parameters), where an individual is a vector of real numbers (the decision variable) and represents a potential solution to the optimization problem. They search for a solution from an initial population (a set of points) that is normally generated at random. In the first and simplest ES, developed by Rechenberg (1984), the selection was made in a population composed of only two members, denoted by the (1 + 1) – ES. In this strategy, at a given generation, there is only one parent (μ = 1) and one offspring (λ = 1) generated by mutation. Selection occurs between the two based on the error function value, provided that it satisfies all constraints. The selected one then becomes the parent of the next generation, and the process is repeated until the stop criteria are met. Later, the same author developed a more complex multi-member strategy where the selection was made on a population of l > 1 parents and one offspring, denominated (μ + 1) – ES. Although this strategy is not widely used, it has led to further enhancements.

Rechenberg (1984) also developed the (μ + λ) – ES, that in a given generation, a population of μ parents generates λ offspring by mutation. Then, the μ parents plus λ offspring are sorted according to their objective function values. Finally, the l parents used in the next generation are the best individuals among the μ parents and the λ offspring (i.e., the selection takes place among the μ + λ members).

The mutation is a genetic operator that creates new points by adding random normal distributed quantities Zk with mean zero and variance. σ_i^2 to the parent (vector of decision variables) in a process called Gaussian mutation. It is important to note that, for each decision variable, an individual standard deviation σ_i can be used (controlling the step sizes). The initial standard deviations for the mutation σ_i can be set using Eq. (1).

$$\sigma_i^{(0)} = \frac{\Delta x}{\sqrt{n}} \tag{1}$$

where Δx is a rough measure of the distance to the optimum and n is the problem dimension. However, it can be not easy to estimate Dx; therefore, the alternative Eq. (1) can be used.

$$\sigma_i^{(0)} = \frac{\beta_i - \alpha_i}{\lambda\sqrt{n}} \tag{2}$$

where α_i and β_i are the lower and upper bounds of the decision variable i. During the search, the standard deviations (or step sizes for mutation) are adapted, and this is one of the most promising features of the ES. They are updated during the process using different rules and self-adaptation schemes, which enhance the algorithm's performance (Rechenberg 1984). Several self-adaptation schemes are possible. For the non-isotropic mutation, where the adopted standard deviations are different for each variable, one possibility is to update these standard deviations. σ_i according to the equation

$$\sigma_i^{(k+1)} = \sigma_i^k e^{Z_i} e^{Z} \tag{3}$$

where $Z_i \sim N(0, \Delta\sigma^2)$, $Z \sim N(0, \Delta\sigma^2)$ which means Z_i and Z follows a normal distribution with zero means and $\Delta\sigma$ and $\Delta\sigma^2$ representing their variance are parameters of the algorithm. Originally, the ES was based only on one operator, mutation, to generate new individuals. Later, Schwefel and Rudolph (1995) reported a remarkable acceleration in the search process, as well as the facilitation of self-adaptation of parameters by introducing a recombination operator. It consists of, before mutation, recombining a set of chosen parents to find a new solution. A given number ρ $(1 \leq \rho \leq \mu)$ of parents are randomly chosen for recombination. When ρ = 1, then there is no recombination. Thus, the nomenclature for the ES can now be extended, and ESs with recombination are usually referred to as (μ / ρ + λ) – ES or (μ / ρ,λ) – ES. There are two main types of recombination, namely intermediate and discrete. In the intermediate recombination, the components

of the offspring are obtained by calculating the average of the corresponding components of the parents (randomly selected from the population). In the discrete recombination, each component of the offspring is chosen from one of the q parents at random. Moth flame optimizer Moths are fancy insects which are highly similar to the family of butterflies. There are over 160,000 various species of this insect in nature. They have two main milestones in their lifetime: larvae and adults. The larvae are transformed into moths by their cocoons. One of the most interesting facts about moths is their unique navigation methods at night. They have evolved to fly at night using the moonlight. They utilized a mechanism called transverse orientation for navigation. In this method, a moth flies by maintaining a fixed angle concerning the moon, a very effective mechanism for traveling long distances in a straight line. Since the moon is far away from the Earth, this mechanism ensures a straight-line flight. Humans can use the same navigation method. Suppose that the moon is on the south side of the sky, and a human wants to go to the east. If he keeps the moon on his left side when walking, he would be able to move toward the east in a straight line. Despite the effectiveness of transverse orientation, we usually observe that moths fly spirally around the lights. Moths are attracted to artificial lights and exhibit such behaviors. This is due to the inefficiency of the transverse orientation, which is only helpful for moving in a straight line when the light source is very far away. When moths see a human-made artificial light, they try to maintain a similar angle with the light to fly in a straight line. Since such a light is extremely close compared to the moon, however, maintaining a similar angle to the light source causes a useless or deadly spiral flight path for moths.

3.3 Moth Flame Optimization (MFO)

The MFO algorithm, introduced by Mirjalili (2015b), is a nature-inspired optimization technique that mimics the navigational behavior of moths in a swarm. These moths, acting as search agents, follow unique night-time navigation strategies. In MFO, candidate solutions are treated as search agents, and their spiral movement is modeled using the following matrix

$$M = \begin{bmatrix} m_{1,1} & m_{1,2} & \dots & m_{1,d} \\ m_{2,1} & \ddots & \ddots & m_{2,d} \\ \vdots & \ddots & \ddots & \vdots \\ m_{n,1} & m_{n,2} & \cdots & m_{n,d} \end{bmatrix} \quad (4)$$

Here, n represents the number of search agents, and d denotes the number of dimensions. It is assumed that each individual has an associated array to store the values of the objective function, as shown below

$$OM = \begin{bmatrix} OM_1 \\ OM_2 \\ \vdots \\ OM_n \end{bmatrix} \quad (5)$$

Another essential component of this algorithm is the *flame*, which is represented in matrix form as shown in Eq. (6)

$$F = \begin{bmatrix} f_{1,1} & f_{1,2} & \dots & f_{1,d} \\ f_{2,1} & \ddots & \ddots & f_{2,d} \\ \vdots & \ddots & \ddots & \vdots \\ f_{n,1} & f_{n,2} & \cdots & f_{n,d} \end{bmatrix} \quad (6)$$

It is assumed that an array exists to store the fitness values of F, as presented below

$$OF = \begin{bmatrix} OF_1 \\ OF_2 \\ \vdots \\ OF_n \end{bmatrix} \quad (7)$$

In the MFO algorithm, F is considered the best position attained by M during the search process. To mathematically represent this behavior, the position of each search agent is updated using the following formula

$$M_i = S(M_i, F_j) \quad (8)$$

Here, M_i represents the i-th search agent, F_j denotes the j-th best position found so far, and S refers to the logarithmic spiral function, which is computed as follows

$$S(M_i, F_j) = D_i \cdot e^{bt} \cdot \cos(2\pi t) + F_j \quad (9)$$

In this context, t is a random number within the range [-1, 1], b is a constant that determines the shape of the logarithmic spiral, and D_i represents the distance between the i^{th} search agent and the j-th flame, defined as follows

$$D_i = |F_j - M_i| \quad (10)$$

In this algorithm, each M is constrained to use only one of the F positions to update its position. An adaptive mechanism is introduced to determine the number of F, as expressed in the following equation

$$Flame\_no = \text{round}\left(n - l \times \frac{n-1}{T}\right) \quad (11)$$

Here, l denotes the current iteration number, and T represents the maximum number of iterations.

3.4 Grasshopper optimization algorithm (GOA)

Numerous swarm-based algorithms have been introduced in the literature to tackle complex and challenging optimization problems across various domains, owing to their simplicity and effectiveness in global optimization. Some of the well-known swarm-based optimization algorithms include but are not limited to, PSO (Eberhart and Kennedy 1995), Ant Colony Optimization (ACO) (Dorigo *et al*. 1996), Flower Pollination Algorithm (FPA) (Yang 2012), Grey Wolf Optimization (GWO) (Mirjalili *et al*. 2014), Ant Lion Optimization (ALO) (Mirjalili 2015a), Moth-Flame Optimization (MFO) Mirjalili (2015b), Dragonfly Algorithm (DA) (Mirjalili 2016), Bat Algorithm (BA) (Cai *et al*. 2016), and Whale Optimization Algorithm (WOA) (Ala'M *et al*. 2018). Nearly tall of these methods were originally designed for continuous optimization problems. They were later adapted

for binary optimization problems, such as feature selection in data classification, where they have demonstrated superior performance.

The GOA, first introduced by Saremi *et al*. (2017), is a recent nature-inspired, population-based algorithm that simulates the behavior of grasshopper swarms in nature. It captures the two key phases of optimization: exploration and exploitation of the search space. The grasshoppers' social interactions represent these phases during their search for food. In the larval stage, the swarm's movement is characterized by slow progress and small steps, whereas, in adulthood, the swarm exhibits long-range and abrupt movements as its defining feature.

Building on the description of grasshoppers, Saremi *et al*. (2017) propose three evolutionary operators for updating the positions of individuals in the swarm: the social interaction operator (S_i), the gravity force operator (G_i), and the wind advection operator (A_i), as presented in Eq. (12).

$$X_i = S_i + G_i + A_i \tag{12}$$

Here, X_i represents the position of the *i*-th grasshopper. Each of these behaviors is mathematically modeled as follows:

The interaction operator is calculated using the formula in Eq. (13) (Saremi *et al*. 2017).

$$S_i = \sum_{\substack{j=1 \\ j\neq i}}^{N} S\left(\left|X_j - X_i\right|\right)\frac{X_j - X_i}{d_{ij}} \tag{13}$$

Where *N* denotes the total number of grasshoppers in the swarm, *d_ij* indicates the distance between the *i*-th and *j*-th grasshoppers, and *S* is a function that defines the strength of the social forces, which is calculated as shown in Eq. (14).

$$S(r) = fe^{-\frac{r}{l}} - e^{-r} \tag{14}$$

Where *f* and *l* are constants representing the intensity of attraction and the attractive length scale, respectively, and *r* is a real value.

However, the authors (Saremi *et al*. 2017) do not consider the gravity operator and assume that the wind direction is always directed towards a target. Consequently, Eq. (12) is modified as follows

$$X_i^d = c\left(\sum_{\substack{j=1 \\ j\neq i}}^{N} c\frac{ub_d - lb_d}{2} S\left(\left|X_j - X_i\right|\right)\frac{X_j - X_i}{d_{ij}}\right) + T_d \tag{15}$$

Where ub_d and lb_d are the upper and lower bounds in the *d*-th dimension, and T_d represents the value of the *d*-th dimension in the target (the best solution found so far). The coefficient *c* reduces the comfort zone in proportion to the number of iterations, as calculated in Eq. (16).

$$c = C_{max} - l\frac{C_{max} - C_{min}}{L} \tag{16}$$

Where C_{max} and C_{min} are the maximum and minimum values, l denotes the current iteration, and L represents the maximum number of iterations. In Saremi *et al*. (2017), they set $C_{min} = 0.00001$ and $C_{max} = 1$.

Eq. (15) demonstrates that the next position of a grasshopper is determined by both its current position and the positions of all other grasshoppers (the first term in Eq. (15)), as well as the position of the target (the second term).

The primary motivation for developing the binary variant of the grasshopper optimization algorithm is the quality of exploration, avoidance of local optima, exploitation, and convergence demonstrated by the GOA algorithm in the paper (Saremi *et al*. 2017). These robust characteristics arise from the high repulsion rate between grasshoppers and their efficient searching abilities in nature.

3.5 League Championship Algorithm (LCA)

In the initialization phase, a league (population) consisting of *L* teams (solutions) is created, and the playing strength (fitness value) of each team is evaluated. When optimizing a function with *n* variables, each team consists of n players, with each player representing a specific variable. During this phase, the teams' initial formations are assigned their starting values.

Next comes the competition phase. According to the league schedule, teams compete in pairs over $S \times (L-1)$ weeks, where *S* is the number of seasons and each week is denoted by *t*. After every match between team *i* and team *j*, the outcome is determined as either a win or a loss—draws are not allowed—based on the teams' playing strengths.

Following each round of competition, a recovery phase ensues. During this phase, teams adjust their formations by considering their current best configuration and the outcomes of the previous week. The LCA employs a greedy selection mechanism: if a new formation yields a better playing strength (i.e., a more optimal solution for the *i-th* team), it replaces the current best formation.

The algorithm continues to evolve the population until a predefined stopping condition is satisfied.

Some of the terms used in this description, such as how the league schedule is generated and how the winning team is determined—require further clarification. These concepts are detailed in the following sections.

3.5.1 Generating a league schedule

To simulate a championship setting where teams compete against one another, the process begins by creating a match schedule for each season. A single round-robin format is employed, meaning every team plays against all other teams once per season.

If the number of teams *L* is even, the total number of matches per season is $L(L-1)/2$, with $L/2$ matches taking place concurrently each week over $(L-1)$ weeks. If L is odd, the season spans *L* weeks, with $(L-1)/2$ matches held each week and one team resting (having no match) per week.

This championship structure is repeated over *S* consecutive seasons (Kashan 2009).

3.5.2 Determining winner/loser

In the LCA, each team competes against other teams, and the result of each match is either a win or a loss—draws

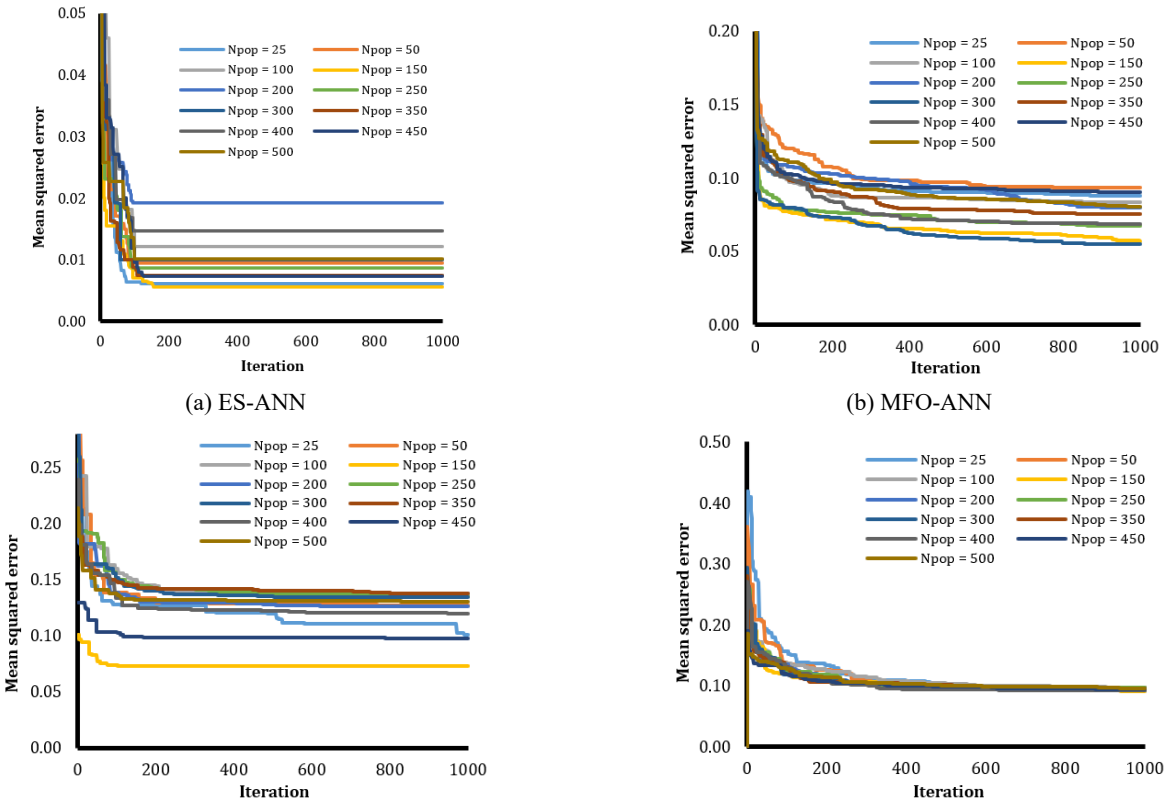

(a) ES-ANN (b) MFO-ANN

(c) GOA-ANN (d) LCA-ANN

Fig. 3 The performance of MSE in order to find the best-fit for each proposed techniques

are not permitted. The outcome of a match is determined probabilistically, with the likelihood of a team winning being proportional to its playing strength. In this context, the playing strength is evaluated based on the team's fitness, meaning teams with higher fitness have a greater chance of winning. As stated by Kashan (2009). "The degree of fit is proportional to the team's playing strength and is measured using the distance from an ideal reference point."

4. Results and discussion

4.1 Optimization of hybrid algorithms

After developing the optimal ANN-based prediction networks, the outputs from each hybrid model were evaluated and compared. This section focuses on identifying the key parameters influencing the performance of the employed optimization algorithms. To assess the effectiveness of each hybrid approach—namely, ES-ANN, MFO-ANN, GOA-ANN, and LCA-ANN—simple and widely used statistical indicators were employed to rank the predicted results against the actual target values. The CRS and TRS ranking methods were employed based on performance metrics, including the coefficient of determination (R^2), mean squared error (MSE), and root mean square error (RMSE).

The outcomes of the performance evaluations are presented in Fig. 3 across a range of population sizes (NP = 25, 50, 75, 100, 150, 200, 250, 300, 350, 400, 450, and 500) and acceleration coefficients. The analysis revealed that ES-ANN achieved its highest accuracy with a population size of 450 (Fig. 3(a)), MFO-ANN at NP = 150 (Fig. 3(b)), GOA-ANN at NP = 250 (Fig. 3(c)), and LCA-ANN at NP = 450 (Fig. 3(d)). These configurations yielded the most accurate predictions of pullout capacity (P_u) for each respective algorithm.

Based on the experimental dataset derived from 36 large-scale laboratory tests and the predictions from the intelligent models, all the proposed hybrid models demonstrated satisfactory performance in estimating P_u. Among them, the MFO-ANN model emerged as the most accurate, outperforming the conventional ANN and other hybrid approaches. This model consistently showed superior results in terms of all statistical indices (e.g., R^2, RMSE) during both the training and testing phases. Specifically, the MFO-ANN achieved R^2 values of 0.9880 and 0.993 and RMSE values of 0.056 and 0.054 for the training and testing sets, respectively, indicating a high degree of accuracy. These findings confirm that the MFO-ANN hybrid model is a robust and reliable tool for accurately predicting the ultimate pullout capacity of belled piles.

The subsequent section presents the training and testing results of the ES-ANN, MFO-ANN, GOA-ANN, and LCA-ANN predictive models in estimating the pullout capacity.

4.2 Model evaluation and presentation

This section evaluates the performance of the two

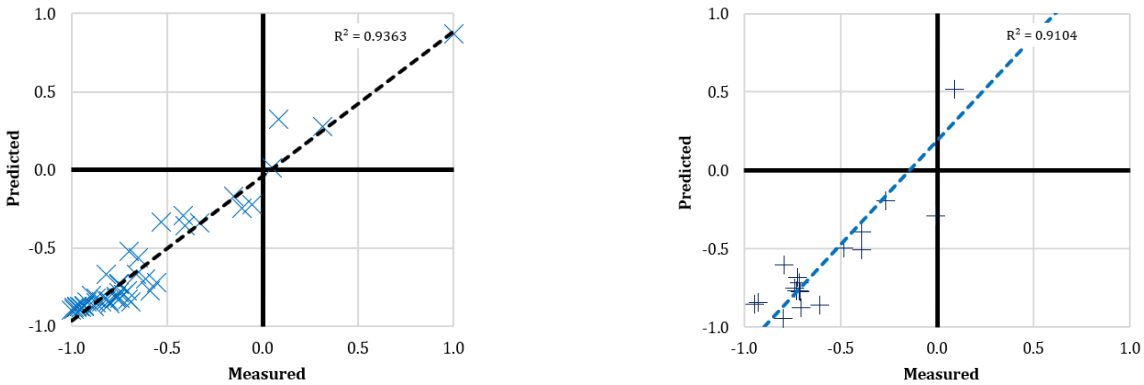

(a) ES-ANN-training

(b) ES-ANN-testing

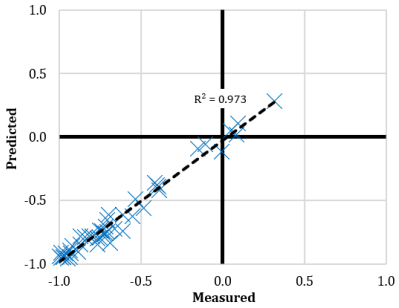

(c) MFO-ANN-training

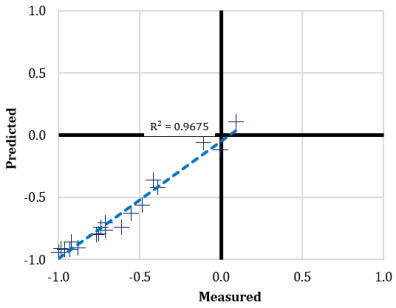

(d) MFO-ANN-testing

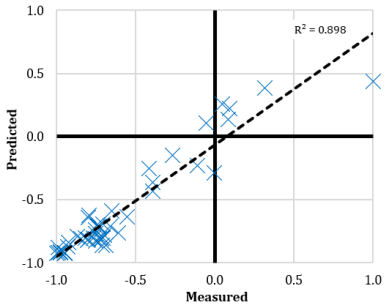

(e) GOA-ANN-training

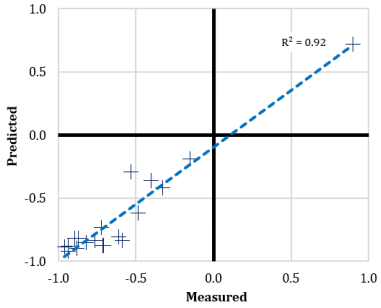

(f) GOA-ANN-training

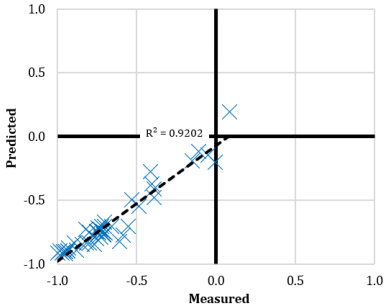

(g) LCA-ANN-training

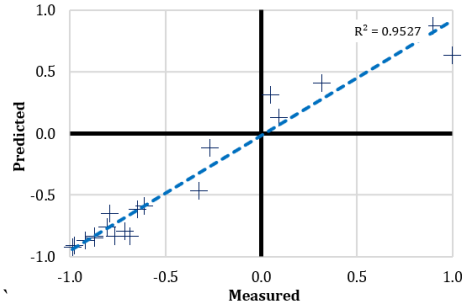

(h) LCA-ANN-training

Fig. 4 Regression results for both the proposed training and testing databases: ES-ANN, MFO-ANN, GOA-ANN, and LCA-ANN

proposed models in estimating the ultimate uplift capacity of belled piles. Fig. 4 illustrates the regression results for both training and testing datasets derived from large-scale laboratory experiments using the ES-ANN, MFO-ANN, GOA-ANN, and LCA-ANN models. The regression analysis between predicted and actual values yields R^2 values of (0.9363, 0.9104), (0.973, 0.9675), (0.898, 0.92), and (0.9202, 0.9527) for the training and testing sets of the ES-ANN, MFO-ANN, GOA-ANN, and LCA-ANN models, respectively.

In the following tables (Tables 2-6), all network results containing R^2 and RMSE should be considered for both training and testing. Finally, according to the total rank, which population size has the most accuracy is assessed. Also, it should be noted that the closer R2 is to 1, the more accurate it is, and for RMSE, Values close to zero indicate

Table 2 Hybrid network results for the ES-ANN

Population size	Network result				Ranking				Total rank	RANK
	Train		Test		Train		Test			
	R^2	RMSE	R^2	RMSE	R^2	RMSE	R^2	RMSE		
25	0.982	0.076	0.882	0.206	11	10	2	6	29	4
50	0.975	0.095	0.940	0.197	8	6	5	7	26	5
100	0.967	0.108	0.972	0.156	3	3	11	9	26	5
150	0.971	0.074	0.924	0.248	7	11	3	3	24	7
200	0.942	0.136	0.924	0.224	1	1	4	4	10	11
250	0.967	0.091	0.965	0.131	4	7	9	10	30	3
300	0.967	0.098	0.746	0.344	5	5	1	1	12	10
350	0.976	0.084	0.946	0.168	9	8	6	8	31	2
400	0.952	0.119	0.971	0.255	2	2	10	2	16	9
450	0.976	0.084	0.953	0.099	10	9	7	11	37	1
500	0.968	0.099	0.954	0.222	6	4	8	5	23	8

Table 3 Hybrid network results for the MFO-ANN

Population size	Network result				Ranking				Total rank	RANK
	Train		Test		Train		Test			
	R^2	RMSE	R^2	RMSE	R^2	RMSE	R^2	RMSE		
25	0.975	0.086	0.934	0.082	2	3	1	2	8	10
50	0.970	0.091	0.975	0.110	1	1	3	1	6	11
100	0.981	0.082	0.991	0.069	4	4	10	7	25	5
150	0.988	0.056	0.993	0.054	11	10	11	10	42	1
200	0.984	0.078	0.985	0.074	5	6	8	6	25	5
250	0.985	0.066	0.981	0.046	7	9	5	11	32	3
300	0.986	0.054	0.984	0.057	9	11	6	9	35	2
350	0.986	0.074	0.973	0.059	8	7	2	8	25	5
400	0.988	0.067	0.987	0.077	10	8	9	4	31	4
450	0.978	0.089	0.985	0.079	3	2	7	3	15	9
500	0.985	0.079	0.978	0.075	6	5	4	5	20	8

greater accuracy. All the total ranks in each table ranged from 1 to 11. As shown in Table 2, for a population size of 450 in the ES-ANN optimization algorithm, the R2 values obtained from training and testing are 0.976 and 0.953, respectively. Also, the results of RMSE obtained from training and testing in this algorithm are 0.084 and 0.099, respectively. It can be seen that the training network accuracies have changed directly in response to the change in population size proposed in the ES-MLP optimization algorithms. For instance, for a population size of 500 compared to 450, the total rank, depending on the ranking of training and testing R^2 and RMSE, is 1 and 4, respectively.

In the MFO-ANN algorithm, as shown in Table 3, for the population size of 150, the R^2 obtained from training and testing are 0.988 and 0.993, respectively. Also, the results of RMSE obtained from training and testing in this algorithm are 0.056 and 0.054, respectively. Although the population size of 300 has better accuracy, according to its good ranking in the R-Square of the training set, it has a lower score compared to the population size of 150, with a ranking of about 1 in the same parameter. According to Table 4, in the GOA-ANN optimization algorithm, for a population size of 250, the R^2 values obtained from training and testing are 0.953 and 0.964, respectively. Also, the results of RMSE obtained from training and testing in this algorithm are 0.132 and 0.090, respectively, for the GOA-ANN optimization algorithm. Training and testing are proposed in Table 4. In which the population size of 250 has a ranking of 1, with a total score of 27. In the LCA-ANN optimization algorithm, for a population size of 450, the R^2 obtained from training and testing is 0.973 and 0.982, respectively (Table 5). Also, the results of RMSE obtained from training and testing in this algorithm are 0.091 and 0.076, respectively. The best score is achieved with a population size of 450, resulting in a total score of 28.

4.3 Discussion

The results of this study provide compelling evidence supporting the use of neural-evolutionary hybrid models in predicting the pullout capacity of belled piles. By integrating artificial neural networks (ANN) with four different optimization algorithms—MFO, LCA, ES, and GOA, the study successfully demonstrated the potential of these models to enhance predictive accuracy and reduce traditional ANN limitations, particularly in cases involving small datasets and complex, nonlinear relationships.

Among the proposed models, MFO-ANN showed the highest predictive accuracy, outperforming the other methods in both RMSE and R^2 metrics. This aligns with findings from previous research, where the Moth Flame Optimizer has demonstrated robust performance in handling high-dimensional, multimodal problems due to its balance between exploration and exploitation. In contrast, the GOA-ANN model, although competitive in terms of global search capability, struggled with fine-tuning toward a unique global optimum in this context. Similar challenges have been reported in other engineering applications, where GOA was efficient in search diversification but less effective in local refinement (Saremi *et al*. 2017). The observed effectiveness of LCA-ANN and ES-ANN models also supports the growing literature on the use of evolutionary strategies and league-based heuristics in engineering optimization. For instance, LCA has been shown to maintain a good balance of convergence speed and solution diversity in structural and geotechnical applications (Kashan 2009), whereas ES-based approaches have a long-standing reputation for stability and adaptability in complex problem spaces (Schwefel and Rudolph 1995).

Moreover, this study reinforces the importance of input parameters such as shaft diameter (Ds), base diameter (Db), soil density, and embedment ratio (L/Db). These factors were also highlighted in earlier empirical and machine learning-based studies as critical influencers of pile

Table 4 Hybrid network results for the GOA-ANN

Population size	Network result				Ranking				Total rank	RANK
	Train		Test		Train		Test			
	R^2	RMSE	R^2	RMSE	R^2	RMSE	R^2	RMSE		
25	0.970	0.099	0.927	0.189	11	9	4	2	26	3
50	0.957	0.125	0.900	0.180	6	6	2	3	17	11
100	0.949	0.135	0.966	0.096	4	1	10	9	24	8
150	0.961	0.071	0.933	0.262	9	11	5	1	26	3
200	0.958	0.124	0.937	0.141	8	7	6	4	25	6
250	0.953	0.132	0.964	0.090	5	3	9	10	27	1
300	0.957	0.132	0.877	0.112	7	4	1	8	20	10
350	0.934	0.135	0.992	0.067	1	2	11	11	25	6
400	0.964	0.117	0.912	0.125	10	8	3	6	27	1
450	0.949	0.096	0.960	0.128	3	10	8	5	26	3
500	0.948	0.128	0.959	0.121	2	5	7	7	21	9

Table 5 Hybrid network results for the LCA-ANN

Population size	Network result				Ranking				Total rank	RANK
	Train		Test		Train		Test			
	R^2	RMSE	R^2	RMSE	R^2	RMSE	R^2	RMSE		
25	0.982	0.077	0.978	0.114	10	9	5	4	28	1
50	0.976	0.086	0.981	0.111	8	7	6	5	26	3
100	0.980	0.077	0.966	0.125	9	8	3	3	23	9
150	0.965	0.087	0.990	0.090	2	6	11	7	26	3
200	0.969	0.093	0.984	0.081	3	3	10	8	24	7
250	0.975	0.100	0.957	0.080	7	1	1	9	18	10
300	0.971	0.090	0.983	0.096	5	5	8	6	24	7
350	0.971	0.096	0.983	0.076	4	2	9	10	25	6
400	0.983	0.068	0.961	0.125	11	11	2	2	26	3
450	0.973	0.091	0.982	0.076	6	4	7	11	28	1
500	0.959	0.076	0.976	0.127	1	10	4	1	16	11

Table 6 Total ranking of best-fitted model for the four employed hybrid methods

Models	Swarm size	Training dataset		Testing dataset		Scoring				Total score	Rank
		RMSE	R^2	RMSE	R^2	Training		Testing			
ESMLP	450	0.084	0.976	0.099	0.953	3	3	1	1	8	3
MFOMLP	150	0.056	0.9880	0.054	0.993	4	4	4	4	16	1
GOAMLP	250	0.132	0.9530	0.09	0.964	1	1	2	2	6	4
LCAMLP	450	0.091	0.9730	0.076	0.982	2	2	3	3	10	2

performance. The ability of the hybrid models, especially MFO-ANN, to extract nonlinear relationships between these parameters and the pullout capacity underlines the adaptability of swarm-based learning methods to geotechnical data.

From a methodological standpoint, the successful application of these models, despite a limited dataset, emphasizes the practicality of hybrid optimization approaches in data-scarce engineering environments. This advantage is significant when compared to conventional regression or standalone artificial neural network (ANN) methods, which often suffer from overfitting or poor generalization under similar conditions. Overall, the findings confirm that hybrid neural-evolutionary models offer a flexible, reliable, and high-performing alternative for modeling complex geotechnical behaviors. With further validation across larger datasets and varied soil conditions, such models could be effectively integrated into modern pile design workflows and decision-support systems.

Similar to Chisari *et al*. (2015), this study also underlines a shared advantage: integrating evolutionary algorithms within model calibration or prediction frameworks significantly improves accuracy, especially in structural systems characterized by nonlinear, multi-variable interactions. Furthermore, while the GA application focused on model updating through experimental-analytical correlation, our approach emphasizes predictive modeling from limited experimental data, suggesting complementary paths for future hybrid methodologies in geotechnical prediction and system identification tasks. Indeed, the present study provides promising insights, and several areas warrant further exploration. First, the relatively small dataset (36 samples) used in this research, though sufficient for initial model training and validation, limits the generalizability of the results. Expanding the dataset—both in terms of quantity and diversity of soil types, loading conditions, and pile geometries—would enable broader validation and refinement of the models. Secondly, while MFO-ANN emerged as the best performer in this case, the relative effectiveness of each hybrid model could vary across different geotechnical scenarios. As such, comparative studies across other types of pile systems, including driven or composite piles, would be beneficial.

Additionally, future work could explore model interpretability through sensitivity analysis or explainable AI techniques to better understand the influence of individual input features on model outputs. This would enhance confidence in using these models for practical decision-making in design. Integrating uncertainty quantification, such as prediction intervals or probabilistic modeling, would also enhance the reliability of predictions in the face of real-world variability.

Also, Young's modulus can significantly enhance the accuracy of bearing capacity predictions. This parameter was excluded from the current model due to limitations in the available dataset. Its inclusion in future studies would strengthen the robustness and generalizability of the predictive models (Chisari *et al*. 2015). This suggestion will be taken into account in the development of extended models that incorporate a broader range of input parameters and alternative optimization algorithms to improve performance and applicability in various geotechnical contexts.

Finally, embedding these hybrid models into user-friendly software platforms or decision support systems could bridge the gap between advanced computational intelligence and engineering practice. The successful translation of these models into design tools would significantly benefit geotechnical engineers tasked with evaluating complex pile behaviors under varied loading and site conditions.

5. Conclusions

In this paper, four hybrid base solutions have been studied to model and predict the influence of several input parameters (e.g., mainly pile geometry) on the ultimate pullout capacity in under-reamed single concrete piles, proving the flexibility, reliability, fast operation, and accuracy of these machine learning methods. Likewise, the laboratory data have mainly depended on the predicted pullout capacity methods, which have mainly depended on shaft diameter (Ds), enlarged base diameter (Db), density condition (i.e., geological ground conditions such as soil density), and penetration depth (or embedment ratio, L/Db). The first objective of this study was to ensure that the neural network can develop a capable predictive method and a feasible design, even when the design problem is highly constrained. It was able to minimize the error by adjusting one of the main input parameters, specifically the swarm size. Consequently, five hybrid techniques of ES-ANN, MFO-ANN, GOA-ANN, and LCA-ANN are implemented to reduce the traditional neural network constraints. As a result, the best predictive network was found for the MFO-ANN (with a swarm size of 150), followed by LCA-ANN, ES-ANN, and GOA-ANN. While GOA-ANN performs well in global search, compared to other proposed hybrid methods, it is weak at fine-tuning (at least for the example provided here) and is designed to

converge to a unique global solution. As demonstrated by the design examples, the proposed hybrid MFO algorithm has potential applications to real-life design problems with different load combinations.

Acknowledgments

Guangzhou Education Bureau's 2024 University Research Project, Research on Intelligent Detection Technology for Underwater Structural Defects Based on Sound Light Fusion (Project Number:2024312299).

Guangzhou Education Bureau's 2024 University Research Project, Study on Aerostatic Interference of Multiple Adjacent Bridges and Their Identification Methods (Project Number:2024312255).

References

Ala'M, A.Z., Faris, H., Alqatawna, J.F. and Hassonah, M.A. (2018), "Evolving support vector machines using whale optimization algorithm for spam profiles detection on online social networks in different lingual contexts", *Knowl.-Based Syst.*, **153**, 91-104. https://doi.org/10.1016/j.knosys.2018.04.025

Amjad, M., Ahmad, I., Ahmad, M., Wróblewski, P., Kamiński, P. and Amjad, U. (2022), "Prediction of pile bearing capacity using XGBoost algorithm: modeling and performance evaluation", *Appl. Sci.*, **12**(4), p. 2126. https://doi.org/10.3390/app12042126

Ashour, M. and Ardalan, H. (2011), "Piles in fully liquefied soils with lateral spread", *Comput. Geotech.*, **38**(6), 821-833. https://doi.org/10.1016/j.compgeo.2011.05.001

Cabalar, A.F., Cevik, A. and Gokceoglu, C. (2012), "Some applications of adaptive neuro-fuzzy inference system (ANFIS) in geotechnical engineering", *Comput. Geotech.*, **40**, 14-33. https://doi.org/10.1016/j.compgeo.2011.09.008

Cai, X., Gao, X.Z. and Xue, Y. (2016), "Improved bat algorithm with optimal forage strategy and random disturbance strategy", *Int. J. Bio-Inspired Computat.*, **8**(4), 205-214. https://doi.org/10.1504/IJBIC.2016.078666

Chang, J., Thewes, M., Zhang, D., Huang, H. and Lin, W. (2024), "Deformational behaviors of existing three-line tunnels induced by under-crossing of three-line mechanized tunnels: a case study", *Can. Geotech. J.*, **62**. https://doi.org/10.1139/cgj-2024-0359

Chisari, C., Bedon, C. and Amadio, C. (2015), "Dynamic and static identification of base-isolated bridges using Genetic Algorithms", *Eng. Struct.*, **102**, 80-92. https://doi.org/10.1016/j.engstruct.2015.07.043

Consoli, N.C., Faro, V.P., Schnaid, F., Born, R.B. and da Silva Carretta, M. (2017), "Crosswise-loaded short and long piles in artificially cemented top sand layers embedded in lightly bonded residual soil", *Soils Foundat.*, **57**(6), 935-946. https://doi.org/10.1016/j.sandf.2017.08.022

Cui, C.Y., Meng, K., Wu, Y.J., Chapman, D. and Liang, Z.M. (2018), "Dynamic response of pipe pile embedded in layered visco-elastic media with radial inhomogeneity under vertical excitation", *Geomech. Eng., Int. J.*, **16**(6), 609-618. https://doi.org/10.12989/gae.2018.16.6.609

Dong, T.W. and Zheng, Y.R. (2015), "Experiment of single screw piles under inclined cyclic pulling loading", *Geomech. Eng., Int. J.*, **8**(6), 801-810. https://doi.org/10.12989/gae.2015.8.6.801

Dorigo, M., Maniezzo, V. and Colorni, A. (1996), "Ant system: optimization by a colony of cooperating agents", *IEEE Transact. Syst. Man Cybernet., Part b* (*Cybernetics*), **26**(1), 29-41. https://doi.org/10.1109/3477.484436

Eberhart, R. and Kennedy, J. (1995), "A new optimizer using particle swarm theory", In: *MHS'95. Proceedings of the 6th International Symposium on Micro Machine and Human Science*, pp. 39-43.

Fleming, W. (1992), "A new method for signle pile settlement prediction and analysis", *Geotechnique*, **42**(3), 411-425. https://doi.org/10.1680/geot.1992.42.3.411

Ganjidoost, H., Mousavi, S.J. and Soroush, A. (2016), "Adaptive network-based fuzzy inference systems coupled with genetic algorithms for predicting soil permeability coefficient", *Neural Processing Letters*, **44**, 53-79. https://doi.org/10.1007/s11063-015-9479-5

Hu, D., Huang, J., Xiang, X., Ni, P., Li, Y., Liang, X. and Liu, J. (2025), "Jacking Force Prediction for Box Jacking Tunnel Considering the Soil Arching Effect", *Int. J. Numer. Anal. Methods Geomech.*, **49**(9), 2161-2176. https://doi.org/10.1002/nag.3979

Hua, L., Tian, Y., Gui, Y., Liu, W. and Wu, W. (2025), "Semi-Analytical Study of Pile–Soil Interaction on a Permeable Pipe Pile Subjected to Rheological Consolidation of Clayey Soils", *Int. J. Numer. Anal. Methods Geomech.*, **49**(3), 1058-1074. https://doi.org/10.1002/nag.3915

Huang, H., Huang, M., Zhang, W. and Yang, S. (2021), "Experimental study of predamaged columns strengthened by HPFL and BSP under combined load cases", *Struct. Infrastr. Eng.*, **17**(9), 1210-1227. https://doi.org/10.1080/15732479.2020.1801768

Kashan, A.H. (2009), "League championship algorithm: a new algorithm for numerical function optimization", In: *2009 International Conference of Soft Computing and Pattern Recognition*, pp. 43-48.

Kumar, A. and Choudhury, D. (2018), "Development of new prediction model for capacity of combined pile-raft foundations", *Comput. Geotech.*, **97**, 62-68. https://doi.org/10.1016/j.compgeo.2017.12.008

Li, W., Wang, G.-G. and Alavi, A.H. (2020), "Learning-based elephant herding optimization algorithm for solving numerical optimization problems", *Knowl.-Based Syst.*, **195**, p. 105675. https://doi.org/10.1016/j.knosys.2020.105675

Liu, F., Yi, J., Cheng, P. and Yao, K. (2020a), "Numerical simulation of set-up around shaft of XCC pile in clay", *Geomech. Eng., Int. J.*, **21**(5), 489-501. https://doi.org/10.12989/gae.2020.21.5.489

Liu, H., Wu, W., Ni, X., Yang, X., Jiang, G., El Naggar, M.H. and Liang, R. (2020b), "Influence of soil mass on the vertical dynamic characteristics of pipe piles", *Comput. Geotech.*, **126**, p. 103730. https://doi.org/10.1016/j.compgeo.2020.103730

Ma, C., Zheng, H., Yang, N., Sun, T., Si, J. and Ren, D. (2025), "Microstructural evolution and mechanical properties of snow under compression", *Constr. Build. Mater.*, **472**, p. 140883. https://doi.org/10.1016/j.conbuildmat.2025.140883

Meng, W., Xin, L., Jinshuai, S., Weiwei, L., Zhongzheng, F., Shuai, W., Jiaxu, K. and Wenguang, Y. (2024), "A study on the reasonable width of narrow coal pillars in the section of hard primary roof hewing along the air excavation roadway", *Energy Sci. Eng.*, **12**(6), 2746-2765. https://doi.org/10.1002/ese3.1799

Mirjalili, S. (2015a), "The ant lion optimizer", *Adv. Eng. Software*, **83**, 80-98. https://doi.org/10.1016/j.advengsoft.2015.01.010

Mirjalili, S. (2015b), "Moth-flame optimization algorithm: A novel nature-inspired heuristic paradigm", *Knowl.-Based Syst.*, **89**, 228-249. https://doi.org/10.1016/j.knosys.2015.07.006

Mirjalili, S. (2016), "Dragonfly algorithm: a new meta-heuristic optimization technique for solving single-objective, discrete, and multi-objective problems", *Neural Comput. Applicat.*, **27**, 1053-1073. https://doi.org/10.1007/s00521-015-1920-1

Mirjalili, S., Mirjalili, S.M. and Lewis, A. (2014), "Grey wolf optimizer", *Adv. Eng. Software*, **69**, 46-61. https://doi.org/10.1016/j.advengsoft.2013.12.007

Moayedi, H. and Rezaei, A. (2019), "An artificial neural network approach for under-reamed piles subjected to uplift forces in dry sand", *Neural Comput. Applicat.*, **31**(2), 327-336. https://doi.org/10.1007/s00521-017-2990-z

Momeni, E., Nazir, R., Armaghani, D.J. and Maizir, H. (2015), "Application of artificial neural network for predicting shaft and tip resistances of concrete piles", *Earth Sci. Res. J.*, **19**(1), 85-93.

Nazir, R., Moayedi, H., Pratikso, A. and Mosallanezhad, M. (2015), "The uplift load capacity of an enlarged base pier embedded in dry sand", *Arab. J. Geosci.*, **8**, 7285-7296. https://doi.org/10.1007/s12517-014-1721-3

Niu, Y., Wang, W., Su, Y., Jia, F. and Long, X. (2024), "Plastic damage prediction of concrete under compression based on deep learning", *Acta Mechanica*, **235**(1), 255-266. https://doi.org/10.1007/s00707-023-03743-8

Ottolini, M., Dijkstra, J. and van Tol, F. (2015), "Immediate and long-term installation effects adjacent to an open-ended pile in a layered clay", *Can. Geotech. J.*, **52**(7), 982-991. https://doi.org/10.1139/cgj-2014-0222

Prendergast, L.J. and Gavin, K. (2016), "A comparison of initial stiffness formulations for small-strain soil–pile dynamic Winkler modelling", *Soil Dyn. Earthq. Eng.*, **81**, 27-41. https://doi.org/10.1016/j.soildyn.2015.11.006

Rechenberg, I. (1984), "The evolution strategy. a mathematical model of darwinian evolution", In: *Synergetics—From Microscopic to Macroscopic Order*: *Proceedings of the International Symposium on Synergetics at Berlin*, July, 1983, pp. 122-132.

Sadeghiamirshahidi, M. and Ardejani, F.D. (2013), "Application of artificial neural networks to predict pyrite oxidation in a coal washing refuse pile", *Fuel*, **104**, 163-169. https://doi.org/10.1016/j.fuel.2012.10.016

Sadrossadat, E., Heidaripanah, A. and Osouli, S. (2016), "Prediction of the resilient modulus of flexible pavement subgrade soils using adaptive neuro-fuzzy inference systems", *Constr. Build. Mater.*, **123**, 235-247. https://doi.org/10.1016/j.conbuildmat.2016.07.008

Saremi, S., Mirjalili, S. and Lewis, A. (2017), "Grasshopper optimisation algorithm: theory and application", *Adv. Eng. Software*, **105**, 30-47. https://doi.org/10.1016/j.advengsoft.2017.01.004

Schwefel, H.-P. and Rudolph, G. (1995), "Contemporary evolution strategies", In: *European Conference on Artificial Life*, pp. 891-907.

Sego, D., Biggar, K. and Wong, G. (2003), "Enlarged base (belled) piles for use in ice or ice-rich permafrost", *J. Cold Regions Eng.*, **17**(2), 68-88. https://doi.org/10.1061/(ASCE)0887-381X(2003)17:2(68)

Thomas, S., Pillai, G.N., Pal, K. and Jagtap, P. (2016), "Prediction of ground motion parameters using randomized ANFIS (RANFIS)", *Appl. Soft Comput.*, **40**, 624-634. https://doi.org/10.1016/j.asoc.2015.12.013

Tu, W., Huang, M., Gu, X. and Chen, H.-P. (2020), "Nonlinear dynamic behavior of laterally loaded composite caisson-piles foundation under scour conditions", *Marine Georesour. Geotech.*, **38**(10), 1265-1280. https://doi.org/10.1080/1064119X.2020.1724217

Wang, J., Zhang, Y., Wang, K., Li, L., Cheng, S. and Sun, S. (2024a), "Development of similar materials with different tension-compression ratios and evaluation of TBM excavation", *Bull. Eng. Geol. Environ.*, **83**(5), p. 190. https://doi.org/10.1007/s10064-024-03674-1

Wang, K., Cao, J., Ye, J., Qiu, Z. and Wang, X. (2024b), "Discrete element analysis of geosynthetic-reinforced pile-supported embankments", *Constr. Build. Mater.*, **449**, p. 138448. https://doi.org/10.1016/j.conbuildmat.2024.138448

Wang, M., Su, J., Qin, H., Shang, L., Kang, J., Liu, W., Li, M., Zhang, F., Li, X. and Fang, Z. (2024c), "Research on active advanced support technology of backfilling and mining face", *Rock Mech. Rock Eng.*, **57**(9), 7623-7642. https://doi.org/10.1007/s00603-024-03808-7

Wang, Y., Han, Z., Xu, X. and Luo, Y. (2024d), "Topology optimization of active tensegrity structures", *Comput. Struct.*, **305**, p. 107513. https://doi.org/10.1016/j.compstruc.2024.107513

Wu, Y., Yamamoto, H. and Yao, Y. (2013), "Numerical study on bearing behavior of pile considering sand particle crushing", *Geomech. Eng., Int. J.*, **5**(3), 241-261. https://doi.org/10.12989/gae.2013.5.3.241

Xiao, J., Yu, Y., Hu, L.Y., Liu, S.B. and Xu, M.H. (2012), "Application of Genetic BP Algorithm in Low Strain Test of Pile Integrity", *Appl. Mech. Mater.*, **101**, 732-736. https://doi.org/10.4028/www.scientific.net/AMM.101-102.732

Yang, X.-S. (2012), "Flower pollination algorithm for global optimization", In: *International Conference on Unconventional Computing and Natural Computation*, pp. 240-249. https://doi.org/10.1007/978-3-642-32894-7_27

Yao, Y., Huang, H., Zhang, W., Ye, Y., Xin, L. and Liu, Y. (2022), "Seismic performance of steel-PEC spliced frame beam", *J. Constr. Steel Res.*, **197**, p. 107456. https://doi.org/10.1016/j.jcsr.2022.107456

Yao, Y., Zhou, L., Huang, H., Chen, Z. and Ye, Y. (2023), "Cyclic performance of novel composite beam-to-column connections with reduced beam section fuse elements", *Structures*, **50**, 842-858. https://doi.org/10.1016/j.istruc.2023.02.054

Yilmaz, I., Marschalko, M., Bednarik, M., Kaynar, O. and Fojtova, L. (2012), "Neural computing models for prediction of permeability coefficient of coarse-grained soils", *Neural Comput. Applicat.*, **21**, 957-968. https://doi.org/10.1007/s00521-011-0535-4

Zhang, Z. and Wang, Y.-H. (2015), "Examining setup mechanisms of driven piles in sand using laboratory model pile tests", *J. Geotech. Geoenviron. Eng.*, **141**(3), p. 04014114. https://doi.org/10.1061/(ASCE)GT.1943-5606.0001252

Zhang, C., Duan, C. and Sun, L. (2024), "Inter-storey isolation versus base isolation using friction pendulum systems", *Int. J. Struct. Stabil. Dyn.*, **24**(02), p. 2450022. https://doi.org/10.1142/S0219455424500226

Zhang, W., Lin, J., Huang, Y., Lin, B. and Liu, X. (2025), "State of the art regarding interface bond behavior between FRP and concrete based on cohesive zone model", *Structures*, **74**, p. 108528. https://doi.org/10.1016/j.istruc.2025.108528

Zhao, J., Tong, H., Yuan, J., Wang, Y., Cui, J. and Shan, Y. (2025), "Three-dimensional strength and deformation characteristics of calcareous sand under various stress paths", *Bull. Eng. Geol. the Environ.*, **84**(1), p. 61. https://doi.org/10.1007/s10064-025-04083-8

Zhou, H., Liu, Z., Shen, W., Feng, T. and Zhang, G. (2022), "Mechanical property and thermal degradation mechanism of granite in thermal-mechanical coupled triaxial compression", *Int. J. Rock Mech. Min. Sci.*, **160**, p. 105270. https://doi.org/10.1016/j.ijrmms.2022.105270

Zhu, M.X., Zhang, Y., Gong, W.M., Wang, L. and Dai, G.L. (2017), "Generalized solutions for axially and laterally loaded piles in multilayered soil deposits with transfer matrix method", *Int. J. Geomech.*, **17**(4), p. 04016104. https://doi.org/10.1061/(ASCE)GM.1943-5622.000080